PERGAMON

International Journal of Solids and Structures 36 (1999) 4071–4087

INTERNATIONAL JOURNAL OF SOLIDS and STRUCTURES

Prediction of overall tension behavior of short fiber-reinforced composites

Zongjin Li[a,*], Bin Mu[a], T. Y. Paul Chang[a], Chin-Tsau Hsu[b]

[a] *Civil and Structural Engineering Department, The Hong Kong University of Science and Technology, Clear Water Bay, Kowloon, Hong Kong*

[b] *Mechanical Engineering Department, The Hong Kong University of Science and Technology, Clear Water Bay, Kowloon, Hong Kong*

Received 6 August 1997; in revised form 16 June 1998

Abstract

The bridging stress of fibers along the crack surface plays an important role in analyzing the tension behavior of short or long fiber-reinforced composites. This paper uses the inclusion theory to obtain the expression of bridging stress for short fiber reinforced composite (SFRC). A simplified model with periodically distributed fibers is proposed to estimate the average fiber spacings. The total fracture resistance is calculated as an energy summation including interface debonding energy dissipation, frictional sliding work between fibers and matrix, strain energy increment of fibers and matrix. The bend over point (BOP) stress is calculated by this fracture resistance. The necessary conditions of the fibers and matrix for the multiple cracking in SFRCs are discussed and the expression of ultimate external stress is derived. The critical fiber volume fraction for the strain hardening response is determined by an iteration method. In the meanwhile, the average spacing between two short fibers is proposed by a periodical distribution assumption. The theoretical prediction is compared with experimental data.

Nomenclature

a	crack radius
d_f	fiber diameter
E_f	Young's modulus of fiber
E_m	Young's modulus of matrix
G_c^M	critical energy release rate of matrix
l	average effective fiber embedded length
k	friction coefficient

* Corresponding author

0020–7683/99/$ - see front matter
PII: S0020–7683(98)00191–7

L_f fiber length
t thickness of the composite plate
V_f volume fractions of fibers
V_f^{cr} the critical value of fiber volume fraction
V_m volume fractions of matrix.

Greek symbols
γ^* debonding surface energy per area
ν_f, ν_m Poisson's ratios of fiber and matrix, respectively
σ_m^u the tension strength of the matrix
τ_f frictional shear stress
τ_u ultimate shear stress.

1. Introduction

It is well recognized that the behavior of tension-weak brittle materials can be improved by the incorporation of high-strength, small-diameter fibers. This toughening effect comes from sliding and debonding between the surface of fibers and matrix which increase the fracture resistance by energy dissipation. From fiber length consideration, there are two kinds of fiber reinforced composites: long and short fiber reinforced composites. Easy processing and low cost compared with continuous long fiber-reinforced composites make the randomly distributed short fiber-reinforced composites become more attractive. Using an extrusion technique, the randomly oriented short fibers can also be aligned approximately in the load direction (Fig. 1). Moreover, with an increase of fiber volume fraction, short fiber reinforced composites can achieve some properties similar to those of long fiber reinforced composites, such as the strain-hardening behavior after the composites' bend over point (Li and Wu, 1992; Li et al., 1993).

Many theoretical models have been presented to predict the tension behavior of fiber reinforced composite (FRC). Most of these models are for continuous long fiber reinforced composites. Marshall et al. (1985) and Marshall and Cox (1987), studied the influence of fiber strength to the tensile fracture behavior of brittle matrix composite based on the theory of micromechanics and fracture mechanics. Aveston et al. (1971) adopted an energy balance method to derive the crack extension stress and used a rule of mixtures (low V_f case) and composite ultimate strength (high V_f case) to determine the critical V_f for multiple cracking to occur. Using the inclusion method, Mori and Mura (1984), Yang et al. (1991), Li et al. (1992, 1993) got the fiber bridging stress expression, and then applied the energy approach to study the fracture behavior of the continuous fiber reinforced composites. For the SFRC case, Li et al. (1991), Wu and Li (1992) and Leung and Li (1991) utilized stress intensity factor and considered snubbing and bundling effects of fibers and a two way debonding to analyze the discontinuous random fiber reinforced composite. The first crack strength has been used by them to determine conditions of multiple cracking.

In the present paper, the inclusion method is used to deduce the relationship of bridging stress and eigenstrain in the crack region for SFRC. The eigenstrain is determined by fracture mechanics consideration. After getting the bridging stress and eigenstrain, the function between the external stress and the total energy release rate of the composites is established. The necessary conditions

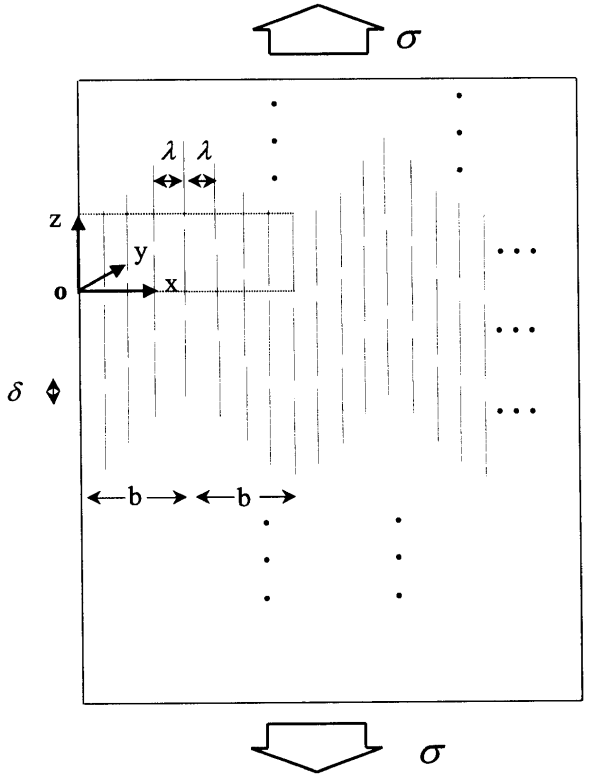

Fig. 1. An infinite aligned short fiber-reinforced composite.

for multiple cracking occurrence are proposed according to equilibrium and maximum strength theories. These conditions seem more reasonable than a single parameter criterion. BOP (at the moment when the first transverse crack happens in composite) and multiple cracking behavior of SFRC are examined using this model. Finally, a comparison between the theoretical and experimental results is presented.

2. Spacing of uniformly distributed short fiber

The configuration of a model of an infinite SFRC under an uniaxial tension loading is shown in Fig. 1. A Cartesian coordinate system (x, y, z) is introduced with the origin located at the point 'o'. In this model, it is supposed that the length and the diameter of the transverse section of each fiber are of the same values denoted by L_f and d_f, respectively; all fibers are extended in the loading direction (z-direction). The spacing of two neighboring fibers in the x-direction and in the z-direction are denoted by λ and δ, respectively. The x and z coordinates of the ends of the fibers falling in a typical section of the model as shown by the dotted line in Fig. 1, are assumed to satisfy a zigzag periodical relation: $z = L_f/b\ x$, for $0 < x < b$, where b is the half period which is supposed to be known. The geometry is also supposed to be independent of y. Thus, by calculating the

volumes of the fibers and matrix (in the range of width b of the dotted line section), the average spacings, λ, δ, satisfy the following equations.

$$V_f = \frac{\frac{1}{4}\pi d_f^2\left[L_f + L_f\left(1-\frac{\lambda}{b}\right) + L_f\left(1-\frac{2\lambda}{b}\right) + \ldots + L_f\left(1-\frac{m\lambda}{b}\right) + n(L_f-\delta)\right]\frac{t}{\lambda}}{b\cdot t\cdot L_f},$$

$$L_f\cdot\frac{m\lambda}{b} = \delta, \quad (m+n) = \frac{b}{\lambda} \tag{1}$$

where V_f and t are the fiber volume fraction and the thickness of the plate, respectively. $m+n+1$ is the number of fibers in the dotted-line section along the x-direction. m defined by the second relationship of eqn (1), is the number of fibers calculated from the second fiber in the dotted-line section along the x-direction to the place where the first fiber of the next row enters into the dotted-line section.

Equation (1) can be rewritten as

$$\lambda = \frac{\pi d_f^2}{16V_f}(2-\phi) + \frac{d_f}{16V_f}\sqrt{\pi^2 d_f^2(2-\phi)^2 + 32V_f\pi(2-2\phi+\phi^2)} \tag{1a}$$

where $\phi = \delta/L_f$. Equation (1a) indicates that λ is a function of δ, i.e. $\lambda = \lambda(\delta)$. On the other hand, δ can be expressed as

$$\delta = \frac{\pi d_f^2}{4V_f\lambda^2}L_f - L_f. \tag{1b}$$

The two unknowns, λ and δ, can be solved from eqns (1a) and (1b). Thus, the distribution of fiber in the matrix can be finally determined. If $\phi \ll 1$, eqn (1a) can be reduced to

$$\lambda \approx \frac{d_f}{2}\sqrt{\frac{\pi}{V_f}}. \tag{1c}$$

Equation (1c) is just the spacing formula of the uniform long fiber reinforced composite for square packing.

For SFRC, the cracks will most likely initiate at an end of fibers (Fig. 2). Generally speaking, the randomly distributed short fibers in a crack have different embedment lengths varying from 0 to $L_f/2$. Those with short embedment length will be pulled out first and stop contributing to bridging the crack openings and the composite load has to be sustained by the remaining bridging fibers. The randomness in fiber embedment lengths should be in an average sense in order to make the analysis rationally sound. Morton (1979) assumed that the average effective embedment length may be estimated from the following equation

$$l = \int_0^{L_f/2} z\frac{2}{L_f}\mathrm{d}z = L_f/4. \tag{2}$$

This assumption was then used by Petersson (1980), and also cited by Li et al. (1991). Their studies and our studies show that eqn (2) is reasonable in practice and may be used as a primary assumption

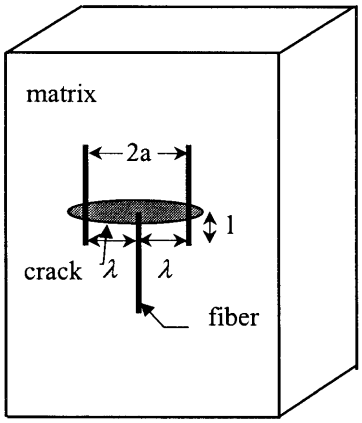

Fig. 2. The crack in the composite.

to analyze the SFRC problem which will be also used in this paper. Note, however, that since the BOP load, the maximum external load and the strain energy of the SFRCs vary nonlinearly with the embedment length, this mean embedment length of $L_f/4$ can only be used as an upper bound estimate to the composite fracture problem as pointed out by Gopalaratnam (1985) and Gopalaratnam and Shah (1987).

3. Bridging stress

Consider a flat ellipsoidal inclusion Ω_0, which approximately represents a penny shape crack in a infinite domain subjected to a uniform tensile stress. Inside the Ω_0, there are a large number of smaller ellipsoidal inclusions, designated by Ω, each of them approximately represents a bridging fiber (Fig. 3). The mathematical expressions of Ω_0 and Ω are

$$\frac{x^2+y^2}{a^2}+\frac{z^2}{c^2}\leqslant 1, \quad \frac{c}{a}\ll 1, \quad \text{for } \Omega_0, \tag{3}$$

$$\frac{x^2+y^2}{\frac{d_f^2}{4}}+\frac{z^2}{c^2}\leqslant 1, \quad \frac{c}{d_f}\ll 1, \quad \text{for } \Omega, \tag{4}$$

where a is the bridged crack radius and $2c$ is the maximum crack opening displacement of the crack.

To simulate the stress in the crack, the strain in the crack area, ε_{zz}, can be expressed as

$$\varepsilon_{zz}=\begin{cases}\varepsilon_p & \in\Omega_0-\Omega\\ \alpha\varepsilon_p & \in\Omega\end{cases} \tag{5}$$

where ε_p is the eigenstrain (Mura 1987) in the matrix and can be evaluated by a matrix failure strain determined later, and α is the bridging factor to characterize the crack opening in the bridged

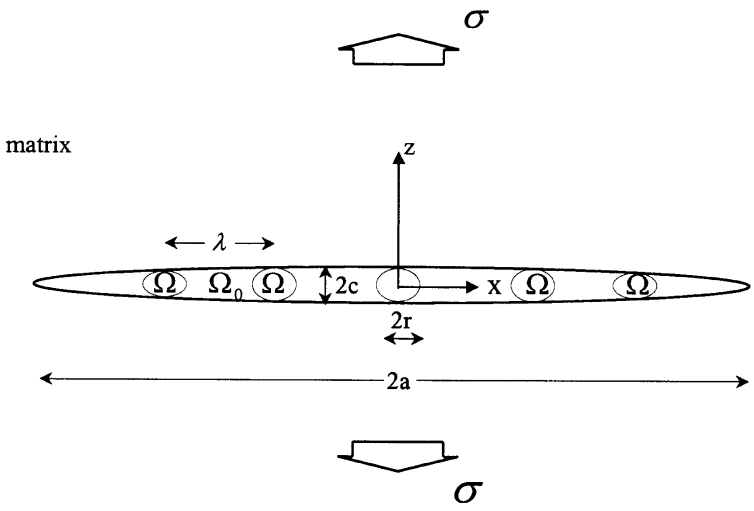

Fig. 3. Ellipsoidal inclusions.

domain Ω, where $0 < \alpha < 1$. For perfect bond between fibers and matrix, $\alpha = 0$; if there exists part debonding or sliding, $0 < \alpha < 1$; for total debonding, $\alpha = 1$.

Using the Green's function given by Mori and Tanaka (1973), Li et al. (1992) obtained the average bridging stress in a fiber which is given by

$$\sigma_T = k_1(1-\alpha) \tag{6}$$

where

$$k_1 = \frac{E_c \pi c \varepsilon_p}{2(1-v_c^2)d_f};$$

E_c, v_c are the average Young's modulus and Poisson's ratio of the composites, respectively.

By the use of shear lag theory and neglecting the interaction between fibers, the stresses in the debonding region were expressed as (Yang et al., 1991)

$$\sigma_f = \sigma_T - \frac{4\tau_f z}{d_f}, \quad \sigma_m = \frac{4\tau_f z V_f}{d_f V_m} \tag{7}$$

where the meaning of z is shown in Fig. 3.

Through the microscopy analysis of the fiber pullout problem, Shao et al. (1993) and Stang et al. (1991) pointed out that the sliding distance l_s can be expressed by

$$l_s = k_2 \sigma_T \tag{8}$$

where

$$k_2 = \frac{d_f}{4\tau_f(1+\eta)},$$

and

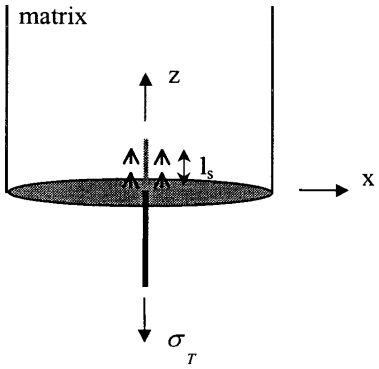

Fig. 4. Debonding of the fiber.

$$\eta = \frac{E_f V_f}{E_m V_m}.$$

The relation of α defined in eqn (6) and the crack opening displacement can be expressed as

$$\Delta_c = 2(u_f - u_m)|_{z=0} = 2c\alpha\varepsilon_p \tag{9}$$

where u_f and u_m are the displacements of fiber and matrix, respectively.

$$u_f = \int_z^{l_s} \frac{\sigma_f}{E_f} dz = \sigma_T \frac{l_s - z}{E_f} - 2\tau_f \frac{l_s^2 - z^2}{d_f E_f}$$

$$u_m = \int_z^{l_s} \frac{\sigma_m}{E_m} dz = 2V_f \tau_f \frac{(l_s^2 - z^2)}{d_f E_m V_m}. \tag{10}$$

Finally, from eqns (6), (8), (9) and (10), the expression for α can be found as,

$$\alpha = \frac{2k_3 + 1 - \sqrt{4k_3 + 1}}{2k_3} \tag{11}$$

where

$$k_3 = \frac{k_1^2 k_2}{E_f c\varepsilon_p}\left(1 - \frac{2\tau_f k_2}{d_f} - \frac{2\tau_f k_2 \eta}{d_f}\right).$$

4. Energy calculation

Having obtained the expression of bridging stress mentioned in the above, the stress in the fiber, σ_f, can be found using the shear lag method (Fig. 4). Suppose $l_s < L_f/4$, otherwise the fiber will be pulled out. Detailed formulation is given in the Appendix. These results are:

$$\sigma_f = \sigma_T - \frac{4}{d_f}\tau_f z, \quad 0 \leqslant z \leqslant l_s, \tag{12}$$

$$\sigma_f = A e^{\sqrt{k_4}z} + B e^{-\sqrt{k_4}z} \frac{k_5}{k_4}\sigma_T, \quad l_s < z \leqslant L_f/4, \tag{13}$$

where

$$k_4 = \frac{4k}{d_f E_f}(1+\eta), \quad k_5 = \frac{4k}{d_f E_f}\eta$$

$$A = k_6\sigma_T - k_7, \quad B = k_8\sigma_T + k_9$$

$$k_6 = \frac{1 - \frac{k_5}{k_4} + \frac{k_5}{k_4} e^{\sqrt{k_4}L_f/4} e^{-\sqrt{k_4}l_s}}{e^{\sqrt{k_4}l_s} - e^{\sqrt{k_4}L_f/2} e^{-\sqrt{k_4}l_s}}$$

$$k_7 = \frac{\frac{4}{d_f}\tau_f l_s}{e^{-\sqrt{k_4}l_s} - e^{\sqrt{k_4}L_f/2} e^{-\sqrt{k_4}l_s}}$$

$$k_8 = \frac{-\left(1 - \frac{k_5}{k_4}\right) e^{\sqrt{k_4}L_f/2} - \frac{k_5}{k_4} e^{\sqrt{k_4}L_f/4} e^{\sqrt{k_4}l_s}}{e^{\sqrt{k_4}l_s} - e^{\sqrt{k_4}L_f/2} e^{-\sqrt{k_4}l_s}}$$

$$k_9 = \frac{\frac{4}{d_f}\tau_f l_s e^{\sqrt{k_4}L_f/2}}{e^{\sqrt{k_4}l_s} - e^{\sqrt{k_4}L_f/2} e^{-\sqrt{k_4}l_s}}.$$

The mechanism of the composite cracks arrested by fibers may be attributed to three kinds of energy consumption: (i) the work done against the frictional sliding, W_s; (ii) the surface energy consumed by the process of debonding, W_d; and (iii) the strain energy increment in the fibers, W_f. The energy release rate is defined by $\Delta G = \partial W/\partial(\pi a^2)$. The results for these energies and the corresponding energy release rates are

$$W_s = 2 \cdot \frac{\pi a^2}{\lambda^2} \cdot \pi d_f \int_0^{l_s} \tau_f (u_f - u_m)\, dz$$

$$= \frac{\pi^2 a^2 d_f \tau_f \sigma_T}{\lambda^2 E_f} l_s^2 - \frac{8\pi^2 a^2 \tau_f^2}{3\lambda^2 E_f}(1+\eta) l_s^3 \tag{14}$$

$$\Delta G_s = \frac{\partial W_s}{\partial(\pi a^2)} = \frac{\pi d_f \tau_f \sigma_T}{\lambda^2 E_f} l_s^2 - \frac{8\pi\tau_f^2}{3\lambda^2 E_f}(1+\eta) l_s^3 \tag{14a}$$

$$W_d = 2 \cdot \frac{\pi a^2}{\lambda^2} \cdot \pi d_f l_s \cdot 2\gamma^* = \frac{4a^2\pi^2 d_f \gamma^* l_s}{\lambda^2} \tag{15}$$

$$\Delta G_{\mathrm{d}} = \frac{4\pi d_{\mathrm{f}}\gamma^* l_{\mathrm{s}}}{\lambda^2} \tag{15a}$$

$$\begin{aligned} W_{\mathrm{f}} &= 2\cdot\frac{\pi a^2}{\lambda^2}\cdot\frac{1}{4}\pi d_{\mathrm{f}}^2\left(\int_0^{l_{\mathrm{s}}}\frac{1}{2}\frac{\sigma_{\mathrm{f}}^2}{E_{\mathrm{f}}}\mathrm{d}z+\int_{l_{\mathrm{s}}}^{L_{\mathrm{f}}/4}\frac{1}{2}\frac{\sigma_{\mathrm{f}}^2}{E_{\mathrm{f}}}\mathrm{d}z\right)\\ &= \frac{\pi^2 a^2 d_{\mathrm{f}}^2}{4E_{\mathrm{f}}\lambda^2}\left(\int_0^{l_{\mathrm{s}}}\sigma_{\mathrm{f}}^2\,\mathrm{d}z+\int_{l_{\mathrm{s}}}^{L_{\mathrm{f}}/4}\sigma_{\mathrm{f}}^2\,\mathrm{d}z\right)\\ &= \frac{\pi^2 a^2 d_{\mathrm{f}}^2}{4E_{\mathrm{f}}\lambda^2}\xi \end{aligned} \tag{16}$$

where

$$\begin{aligned} \xi = &\left[\frac{k_5^2\sigma_{\mathrm{T}}^2 L_{\mathrm{f}}}{4k_4^2}+\frac{L_{\mathrm{f}}}{2}(k_6\sigma_{\mathrm{T}}-k_7)(k_8\sigma_{\mathrm{T}}+k_9)\right]+\left[\sigma_{\mathrm{T}}^2-\frac{k_5^2}{k_4^2}\sigma_{\mathrm{T}}^2-2(k_6\sigma_{\mathrm{T}}-k_7)(k_8\sigma_{\mathrm{T}}+k_9)\right]\cdot l_{\mathrm{s}}\\ &-\frac{4}{d_{\mathrm{f}}}\sigma_{\mathrm{T}}\tau_{\mathrm{f}} l_{\mathrm{s}}^2+\frac{16\tau_{\mathrm{f}}^2}{3d_{\mathrm{f}}^2}l_{\mathrm{s}}^3+\frac{2k_5\sigma_{\mathrm{T}}}{\sqrt{k_4}k_4}(k_6\sigma_{\mathrm{T}}-k_7)(\mathrm{e}^{\sqrt{k_4}L_{\mathrm{f}}/4}-\mathrm{e}^{\sqrt{k_4}l_{\mathrm{s}}})\\ &-\frac{2k_5\sigma_{\mathrm{T}}}{\sqrt{k_4}k_4}(k_8\sigma_{\mathrm{T}}+k_9)(\mathrm{e}^{-\sqrt{k_4}L_{\mathrm{f}}/4}-\mathrm{e}^{\sqrt{k_4}l_{\mathrm{s}}})+\frac{1}{2k_4}(k_6\sigma_{\mathrm{T}}-k_7)^2(\mathrm{e}^{\sqrt{k_4}L_{\mathrm{f}}/2}-\mathrm{e}^{2\sqrt{k_4}l_{\mathrm{s}}})\\ &-\frac{1}{2k_4}(k_8\sigma_{\mathrm{T}}+k_9)^2(\mathrm{e}^{-\sqrt{k_4}L_{\mathrm{f}}/2}-\mathrm{e}^{-2\sqrt{k_4}l_{\mathrm{s}}}) \end{aligned}$$

and

$$\Delta G_{\mathrm{f}} = \frac{\partial W_{\mathrm{f}}}{\partial(\pi a^2)} = \frac{\pi d_{\mathrm{f}}^2}{4E_{\mathrm{f}}\lambda^2}\xi. \tag{16a}$$

The coefficient '2' at the beginning of the right hand side of eqns (14), (15) and (16), is due to the sliding and debonding in both the upper and lower parts of the fibers, and the following $\pi a^2/\lambda^2$ is the number of fibers in the crack region.

5. Criterion for BOP

If no fiber exists in the composites, i.e. plain matrix, the stress intensity factor K_{I} is only dependent on the applied load and structural geometry. For infinite structures, we have

$$K_{\mathrm{I}} = 2\sqrt{\frac{a}{\pi}}\sigma \tag{17}$$

and,

$$G = \frac{1-\nu_m^2}{E_m} K_I^2 \tag{18}$$

where G is the strain energy release rate for plane strain case (Aveston et al., 1971). E_m and γ_m are the Young's modulus and Poisson's ratio of the matrix, respectively.

According to the Griffith criterion, when $G > G_c^M$, a crack will propagate. Here, G_c^M is the critical energy release rate that is a material constant of the matrix. For a given crack radius, a, the critical stress, σ_{cr}, can be expressed by

$$\sigma_{cr} \geqslant \sqrt{\frac{\pi E_m G_c^M}{4a(1-\nu_m^2)}} \tag{19}$$

and, the corresponding failure strain is

$$\varepsilon^* = \frac{\sigma_{cr}}{E_m} = \sqrt{\frac{\pi G_c^M}{4aE_m(1-\nu_m^2)}}. \tag{20}$$

When the external stress exceeds the critical value, the crack will propagate for a plain matrix. The value of G_c^M can be obtained from the experiment (Ouyang and Shah, 1991). However, with the presence of fibers, the materials become tougher, because the resistance due to energy dissipation is increased. The new fracture resistance becomes

$$R = G_c^M + \Delta G_s + \Delta G_d + \Delta G_f. \tag{21}$$

For composites, eqn (18) is still applicable (Mori and Mura, 1984), and it can be rewritten as

$$R = \frac{1-\nu_c}{E_c} K_I^2. \tag{22}$$

So, the applied external stress at the BOP (when the first transverse crack happens) of the composites is

$$\sigma = \sqrt{\frac{\pi E_c (G_c^M + \Delta G_s + \Delta G_d + \Delta G_f)}{4a(1-\nu_c^2)}} \tag{23}$$

where E_c and γ_c are the Young's modulus and Poisson's ratio of the composite, respectively.

6. Multiple cracking

For fiber reinforced composites, two possibilities exist after the formation of the first transverse crack: strain softening characterized by continuous opening of the major crack due to fiber pull-out and strain hardening characterized by multiple cracking. For fiber reinforced cementitious composites, the multiple cracking is described as a second or more cracks propagate along the transverse direction, i.e. x-direction (Fig. 1), parallel to the first transverse crack (Gopalaratnam and Shah, 1987; Li and Leung, 1992; Li et al., 1993). According to this definition, three conditions

have to be satisfied in order to let multiple cracking occur. First, the failure force of the fibers in the crack area should be larger than the first transverse crack force (BOP force), P^{BOP}, i.e.

$$\sigma_{\mathrm{f}}^{\mathrm{u}} V_{\mathrm{f}} A_{\mathrm{c}} \geqslant P^{\mathrm{BOP}} \tag{24}$$

where A_{c} is the transverse surface of the first crack and $\sigma_{\mathrm{f}}^{\mathrm{u}}$ is the strength of the fiber, otherwise the fibers will be broken at the BOP and no multiple cracking happens.

Second, the tensile stresses re-built up in the matrix have to exceed the tensile strength of the matrix. This also means that the total bond strength of a fiber between two cracks should be larger than the matrix tensile strength, i.e.

$$\frac{\left(\int_{l_{\mathrm{s}}}^{L/4} 4\tau \,\mathrm{d}l + 4\tau_{\mathrm{f}} l_{\mathrm{s}}\right) \cdot V_{\mathrm{f}}}{d_{\mathrm{f}} \cdot V_{\mathrm{m}}} \geqslant \sigma_{\mathrm{m}}^{\mathrm{u}} \tag{25}$$

where $\sigma_{\mathrm{m}}^{\mathrm{u}}$ is the strength of the matrix and τ can be calculated from the eqn (A1) in the Appendix.

Finally, the total bond force of the fiber should be greater than the first transverse crack force, i.e.

$$\sum\left[\int_{l_{\mathrm{s}}}^{L/4} \tau \pi d_{\mathrm{f}} \,\mathrm{d}l + \tau_{\mathrm{f}} \pi d_{\mathrm{f}} l_{\mathrm{s}}\right] \geqslant P^{\mathrm{BOP}} \tag{26}$$

otherwise the fibers will be pulled out.

Suppose a fiber along the crack surface is under a tension stress, σ^*, then by using shear strength criterion (Appendix) and letting the shear stress of the matrix equal τ_{u} at $z = l_{\mathrm{s}}$, we get the following relationship

$$\sigma^* = \frac{4\tau_{\mathrm{u}} - d_{\mathrm{f}}\sqrt{k_4}(k_7 \mathrm{e}^{\sqrt{k_4} l_{\mathrm{s}}} + k_9 \mathrm{e}^{-\sqrt{k_4} l_{\mathrm{s}}})}{d_{\mathrm{f}}\sqrt{k_4}(k_8 \mathrm{e}^{-\sqrt{k_4} l_{\mathrm{s}}} - k_6 \mathrm{e}^{\sqrt{k_4} l_{\mathrm{s}}})}. \tag{27}$$

In eqn (27), l_{s} increases as σ^* increases, however there exists a critical debonding length l^*, beyond which the debonding process would be catastrophic. By setting $\mathrm{d}\sigma^*/\mathrm{d}l_{\mathrm{s}} = 0$, this critical debonding length together with the ultimate external stress can be expressed as

$$l_{\mathrm{s}}^* \approx \frac{L_{\mathrm{f}}}{4} - \frac{1}{\beta} \cosh^{-1} \sqrt{\frac{\tau_{\mathrm{u}}}{\tau_{\mathrm{f}}}} \tag{28}$$

$$\sigma^{\mathrm{u}} = \frac{4\tau_{\mathrm{f}} l_{\mathrm{s}}^* V_{\mathrm{f}}}{d_{\mathrm{f}}} + \frac{4\tau_{\mathrm{u}} V_{\mathrm{f}}}{d_{\mathrm{f}} \beta} \tanh \beta \left(\frac{L_{\mathrm{f}}}{4} + l_{\mathrm{s}}^*\right) \tag{29}$$

where

$$\beta = \sqrt{\frac{\pi E_{\mathrm{m}}}{(1+\nu_{\mathrm{m}}) A_{\mathrm{f}} E_{\mathrm{f}} \ln\left(\frac{1}{2}\sqrt{\frac{\pi}{V_{\mathrm{f}}}}\right)}}$$

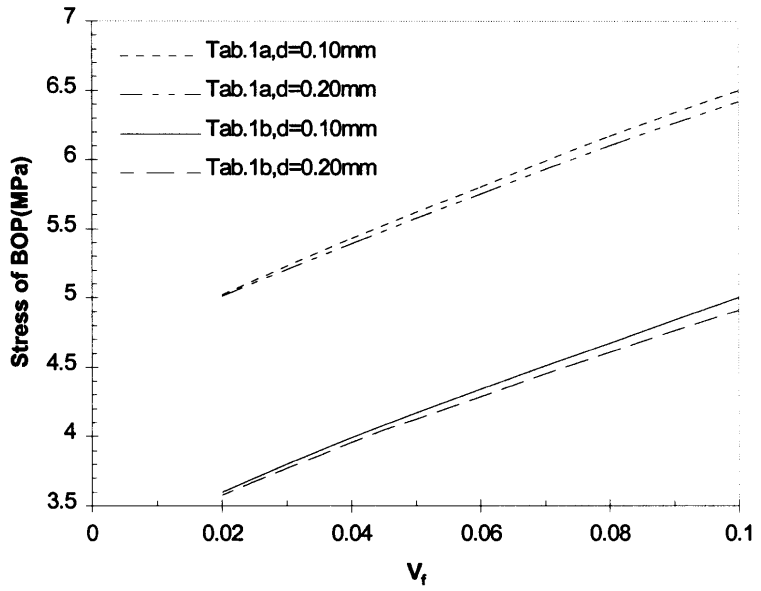

Fig. 5. BOP stresses of various fiber volume fractions and diameters ($L_f = 10$ mm).

and σ^u is the ultimate external stress which leads to the fibers being pulled out from the matrix, assuming that the fibers are strong enough that they will not be broken in the loading process.

7. Results and discussion

The influence of fiber volume fractions and fiber diameters on BOP is shown in Fig. 5. The stress values of BOP of the plain matrix are about 4.6 and 3.2 MPa as shown in Table 1, values (a) and (b) respectively. When fibers are added, the stresses of BOP increase with the increase of the fiber

Table 1
Material properties and interfacial parameters

Item	Value (a)	Value (b)
Mix design	C : S : W (1 : 2 : 0.5)	C : W (1 : 0.35)
Elastic modulus of matrix	20 GPa	14 GPa
Elastic modulus of fiber	200 GPa	200 GPa
Days of aging	28	14
Surface energy of matrix	22 N m^{-1}	15 N m^{-1}
Surface energy of interface	8 N m^{-1}	5.5 N m^{-1}
Friction shear stress	1.9 MPa	1.30 MPa
Ultimate shear stress	2.74 MPa	1.92 MPa
Friction coefficient	4.22×10^{10} N m^{-3}	2.95×10^{10} N m^{-3}

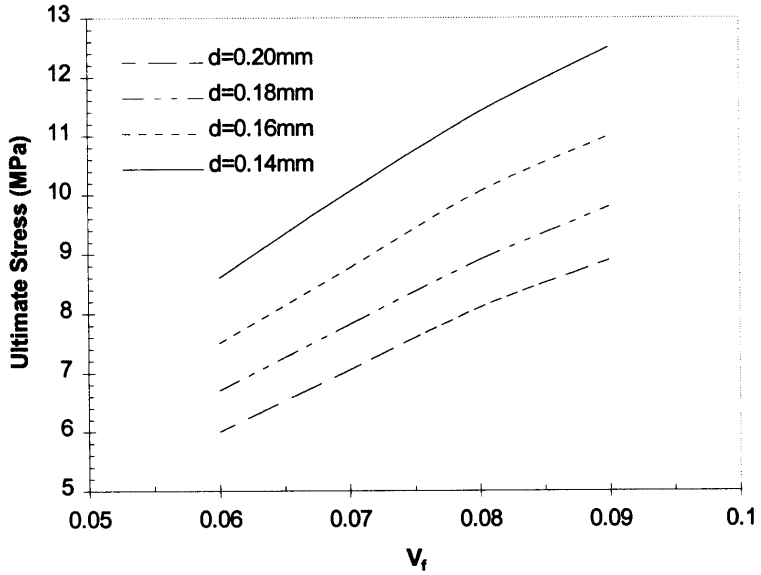

Fig. 6. Ultimate stresses of various fiber volume fractions and diameters ($L_f = 10$ mm).

volume fractions as can be seen in Fig. 5. When $V_f = 10\%$, the stresses of BOP are 40–60% higher than those of the plain matrix, depending on fiber diameter. Figure 5 also shows that matrix with different material properties (Table 1a and 1b) can cause different bridging effects, although the fiber diameters are the same.

The influence of fiber parameters on BOP stresses and ultimate stresses is quite different as can be found in Figs 5 and 6. The BOP stresses calculated by eqn (23) do not seem to alter very much with the different fiber diameters (Fig. 5). However, they have significant influence on the ultimate external stresses of the composites as calculated by eqn (29) (Fig. 6). For the four different diameters in Fig. 6, when $V_f = 9\%$, the strength with $d_f = 0.14$ mm is about 40% greater than that with $d_f = 0.20$ mm. The reason is, that if the fiber volume ratio keeps constant, the increase of the fiber diameters will increase the spacing of fibers. This implies that the fibers become sparser in the composites. As a result, the bridging effects are degraded.

As is well known, for a cementitious fiber-reinforced composite, there exists a critical fiber volume ratio, beyond which only the strain hardening or multiple cracking happens. In this paper, the critical values of the fiber volume fractions with different fiber diameters are presented in Fig. 7. They can be calculated by a numerical iteration method using the criterion based on the fact that the ultimate external stress should be larger than the BOP stress.

$$\sigma^{u} \geqslant \sigma \tag{30}$$

where σ is defined in eqn (23) and σ^{u} is given in eqn (29). The material parameters used for Figs 6 and 7 are from Table 1, value (a).

Different mixing formulas have different interface properties and these properties directly influence the mechanical behavior of SFRC. Figure 8 plots the ultimate stresses as a function of fiber

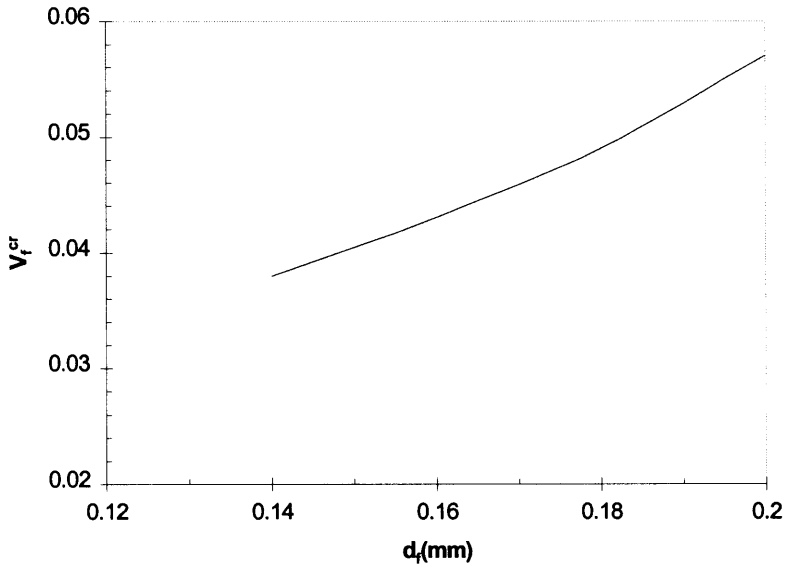

Fig. 7. Critical fiber volume fractions of various fiber diameters ($L_f = 10$ mm).

volume ratios. It can be seen from the figure that the ultimate stress is significantly increased when the interfacial bond becomes stronger.

To verify the applicability of the model presented in this paper, some theoretical results have been compared with the experimental results. Figure 9 shows the comparison of BOP between the

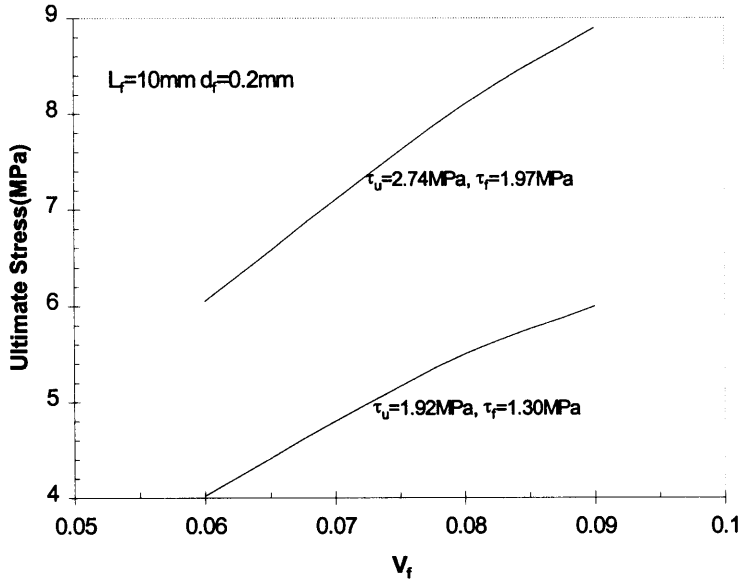

Fig. 8. Ultimate stresses with different interfaces of fiber and matrix.

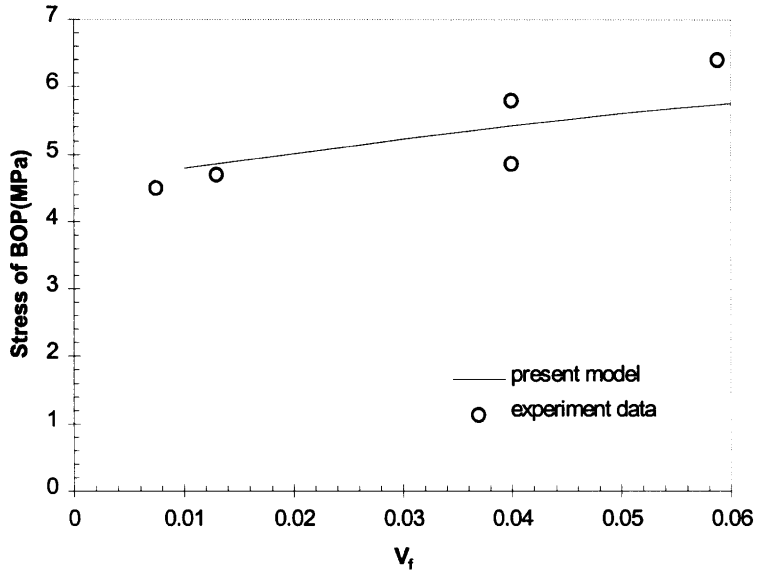

Fig. 9. Comparison of predicted and experiment results ($d_f = 0.2$ mm).

prediction of the present study and experimental results (Li et al., 1992; Shao et al., 1993; Lange et al., 1996). The material properties and interfacial parameters for this kind of composite are listed in Table 1 given by Li et al. (1991) and Li et al. (1992). The theoretical prediction reasonably agrees with the experimental results.

8. Conclusion

The mechanism of fiber-reinforced composites depends on many factors such as fiber and matrix properties, interfacial characterizations and processing methods. For the strain hardening type of composites, the stress–strain curve can be divided into four stages, random damage distribution, BOP, multiple cracking and only fiber sustaining any additional load. The enhanced toughness and load carrying capability can be largely attributed to the fiber bridging, interfacial debonding and sliding.

Based on the energy approach and the inclusion method, a theoretical model to predict the BOP stress of the SFRC has been developed in this paper. It also provides the conditions for multiple cracking. The model is simple and has been applied to SFRC successfully. In addition, this model can be extended to analyze continuous long fiber reinforced composites.

Acknowledgements

The financial support of the grant HKUST 641/95E from the Research Grants Council of the Hong Kong government is greatly acknowledged. Special thanks are also given to Dr Z. L. Li for his helpful suggestions and discussions.

Appendix

Relationship between σ_f and σ_T

From Fig. 4, considering the chemical bond in the interfacial of matrix and fibers, the shear stress can be described as

$$\tau = \begin{cases} k(u_m - u_f) & \tau < \tau_u \\ \tau_f & \tau \geqslant \tau_u \end{cases}. \tag{A1}$$

The equilibrium equation of fiber stress and interfacial shear stress is

$$\frac{\partial \sigma_f}{\partial z} + \frac{4}{d_f}\tau = 0. \tag{A2}$$

Neglecting the interaction between the fibers, the global equilibrium equation is

$$V_f \sigma_T = V_f \sigma_f + V_m \sigma_m. \tag{A3}$$

Combining eqns (A1), (A2) and (A3), together with

$$\frac{\partial u_f}{\partial z} = \frac{\sigma_f}{E_f} \quad \text{and} \quad \frac{\partial u_m}{\partial z} = \frac{\sigma_m}{E_m},$$

the following differential equation can be deduced:

$$\frac{\partial^2 \sigma_f}{\partial z^2} - k_4 \sigma_f = -k_5 \sigma_T \tag{A4}$$

where k_4 and k_5 are defined in eqn (13).

By the boundary conditions, σ_f continuous at $z = l_s$; and $\sigma_f = 0$ at $z = L_f/4$, eqn (A4) can be solved and eqn (13) is obtained.

References

Aveston, J., Cooper, G.A., Kelly, A., 1971. Single and Multiple Fracture. In: Proceedings of The Properties of Fibre Composites. National Physical Laboratory IPC Science and Technology Press, U.K. pp. 15–24.

Gopalaratnam, V.S., 1985. Fracture and impact resistance of steel fiber reinforced concrete. PhD. thesis Northwestern University, Evanston, IL.

Gopalaratnam, V.S., Shah, S.P., 1987. Tensile failure of steel fiber-reinforced mortar. Journal of Engineering Mechanics 113, 635–652.

Lange, D.A., Ouyang, C., Shah, S.P., 1996. Behavior of cement based matrices reinforced by randomly dispersed microfibers. Advanced Cement Based Materials 3, 20–30.

Leung, C.K., Li, V.C., 1991. New strength-based model for the debonding of discontinuous fibers in an elastic matrix. Journal of Materials Science 26, 5996–6010.

Li, V.C., Leung, C.K., 1992. Steady-state and multiple cracking of short random fiber composites. Journal of Engineering Mechanics 118, 2246–2264.

Li, V.C., Wu, H.C., 1992. Conditions for pseudo strain-hardening in fiber reinforced brittle matrix composites. Appl. Mech. Rev. 45, 390–398.

Li, Z., Mobasher, B., Shah, S.P., 1991. Characterization of interfacial properties in fiber-reinforced cementitious composites. Journal of the American Ceramic Society 74, 2156–2164.

Li, V.C., Wang, Y., Backer, S., 1991. A micromechanical model of tension-softening and bridging toughening of short random fiber reinforced brittle matrix composites. Journal of the Mechanics and Physics of Solids 39, 607–625.

Li, S.H., Li, Z., Mura, T., Shah, S.P., 1992. Multiple fracture of fiber-reinforced brittle matrix composites based on micromechanics. Engineering Fracture Mechanics 43, 561–579.

Li, S.H., Shah, S.P., Li, Z., Mura, T., 1993. Micromechanical analysis of multiple fracture and evaluation of debonding behavior for fiber-reinforced composites. International Journal of Solids and Structures 30, 1429–1459.

Marshall, D.B., Cox, B.N., 1987. Tensile fracture of brittle matrix composites: Influence of fiber strength. Acta Metall. 35, 2607–2619.

Marshall, D.B., Cox, B.N., Evans, A.G., 1985. The mechanics of matrix cracking in brittle-matrix fiber composites. Acta Metall. 33, 2013–2021.

Mori, T., Mura, T., 1984. An inclusion model for crack arrest in fiber reinforced materials. Mechanics of Materials 3, 193–198.

Mori, T., Tanaka, K., 1973. Average stress in matrix and average elastic energy of materials with misfitting inclusions. Acta Metall. 21, 571–574.

Morton, J., 1979. Materiaux et Constructions 12, 393.

Mura, T., 1987. Micromechanics of Defects in Solids. Martinus Nijhoff Publishers, Dordrecht.

Ouyang, C., Shah, S.P., 1991. Geometry-dependent R-curve for quasi-brittle materials. Journal of the American Ceramic Society 74, 2831–2836.

Petersson, P.E., 1980. Fracture mechanical calculations and tests for fiber-reinforced cementitious materials. In: Proceedings of Advances in Cement Matrix Composites, MRS meeting, Boston, pp. 95–106.

Shao, Y., Li, Z., Shah, S.P., 1993. Matrix cracking and interface debonding in fiber-reinforced cement-matrix composite. Journal of ACBM 1, 55–66.

Stang, H., Li, Z., Shah, S.P., 1991. Pullout problem: Stress versus fracture mechanical approach. Journal of Engineering Mechanics 116, 2136–2150.

Wu, H.C., Li, V.C., 1992. Snubbing and bundling effects on multiple crack spacing of discontinuous random fiber-reinforced brittle matrix composites. Journal of the American Ceramic Society 75, 3487–3489.

Yang, C.C., Mura, T., Shah, S.P., 1991. Micromechanical theory and uniaxial tensile tests of fiber reinforced cement composites. Journal of Materials Research 6, 2463–2473.